ARTHRITIS & RHEUMATOLOGY
Vol. 67, No. 1, January 2015, pp 74–85
DOI 10.1002/art.38878

Expression and Function of Aminopeptidase N/CD13 Produced by Fibroblast-like Synoviocytes in Rheumatoid Arthritis

Role of CD13 in Chemotaxis of Cytokine-Activated T Cells Independent of Enzymatic Activity

Rachel Morgan, Judith Endres, Nilofar Behbahani-Nejad, Kristine Phillips, Jeffrey H. Ruth, Sean C. Friday, Gautam Edhayan, Thomas Lanigan, Andrew Urquhart, Kevin C. Chung, and David A. Fox

Objective. **Aminopeptidase N/CD13 (EC 3.4.11.2) is a metalloproteinase expressed by fibroblast-like synoviocytes (FLS). It has been suggested that CD13 can act chemotactically for T cells in rheumatoid arthritis (RA). We undertook this study to measure CD13 in vivo and in vitro in RA samples and to determine whether CD13 could play a role in the homing of T cells to the RA joint.**

Methods. **Interleukin-17–treated FLS were used to immunize mice, from which a novel anti-human CD13 monoclonal antibody (mAb), 591.1D7.34, was developed. The mAb 591.1D7.34 and a second anti-CD13 mAb, WM15, were used to develop a novel enzyme-linked immunosorbent assay (ELISA) for CD13, and CD13 enzymatic activity was measured in parallel. Chemotaxis of cytokine-activated T cells was measured by a chemotaxis-under-agarose assay.**

Results. **We detected substantial amounts of CD13 in synovial fluid (SF), sera, FLS lysates, and culture supernatants by ELISA, with a significant increase in CD13 in RA SF when compared to osteoarthritis SF. CD13 accounted for most but not all of the CD13-like enzymatic activity in SF. Recombinant human CD13 was chemotactic for cytokine-activated T cells through a G protein–coupled receptor and contributed to the chemotactic properties of SF independently of enzymatic activity.**

Conclusion. **CD13 is released from FLS into culture supernatants and is found in SF. CD13 induces chemotaxis of cytokine-activated T cells, a T cell population similar to that found in RA synovium. These data suggest that CD13 could play an important role as a T cell chemoattractant, in a positive feedback loop that contributes to RA synovitis.**

Aminopeptidase N/CD13 (EC 3.4.11.2) is a metalloproteinase of the M1 family (1–4). It can be found on the membrane of many cell types (including cells of monocytic lineage and fibroblasts) and also as a truncated soluble protein (2–6). CD13 is a Zn^{2+}-dependent ectoenzyme that cleaves the N-terminal peptide off substrates preferentially after a neutral amino acid (2–4). Substrates of CD13 include enkephalins, angiotensins, neurokinins, chemokines, and cytokines, and CD13 may degrade various extracellular matrix (ECM) components, aiding in cellular migration (2–4,7,8). CD13 has also been linked to immune-mediated conditions including rheumatoid arthritis (RA), scleroderma, psoriasis, and chronic graft-versus-host disease (2–4,9–12).

RA is an autoimmune disease characterized by synovial inflammation and ultimately destruction of bone and cartilage. Infiltration of lymphocytes is one essential component of RA synovitis (13). In synovial

Supported by the NIH (grant R01-F018446-05, Research Supplements to Promote Diversity in Health-Related Research grant 10-PAF00195, and Training Grant in Experimental Immunology 2T32-A1007413-16).

Rachel Morgan, BS, Judith Endres, BSc, Nilofar Behbahani-Nejad, MS, Kristine Phillips, MD, PhD, Jeffrey H. Ruth, PhD, Sean C. Friday, PhD, Gautam Edhayan, BSE, Thomas Lanigan, PhD, Andrew Urquhart, MD, Kevin C. Chung, MD, MS, David A. Fox, MD: University of Michigan, Ann Arbor.

Address correspondence to David A. Fox, MD, Division of Rheumatology, University of Michigan, North Ingalls Building, Room 7C27, 300 North Ingalls Street, Ann Arbor, MI 48109-5422. E-mail: dfox@med.umich.edu.

Submitted for publication June 2, 2014; accepted in revised form September 9, 2014.

tissue, T cells can interact with other cells (including fibroblast-like synoviocytes [FLS], macrophages, B cells, and dendritic cells), leading to cell activation and cytokine secretion (13–15). Various chemokines have been proposed to attract T cells to the RA joint including thymus and activation–regulated chemokine (TARC)/CCL17, interleukin-8 (IL-8)/CXCL8, stromal cell–derived factor 1 (SDF-1)/CXCL12, and macrophage inflammatory protein 1α/CCL3 (15–17). CD13 involvement in RA has been previously suggested, and phenomena that can be functionally linked to CD13 are seen in RA (angiogenesis, cellular migration, and monocyte activation) (2–4,10). However, a definitive role for CD13 in RA has not been shown, and the protein has not been directly measured. Enzymatic assays of CD13 activity and chemical inhibition of its enzymatic activity have been used, but neither the assays nor the inhibitors of CD13 are specific for CD13 versus other aminopeptidases (18). Our goals in this study were to measure CD13 protein in RA and to test the hypothesis that CD13 in synovial fluid (SF) is chemotactic for T cells. The results identify soluble CD13 (sCD13) as a protein that is preferentially produced in the RA joint and has chemotactic effects on a population of T cells that are similar to RA synovial T cells, at concentrations found in SF in vivo.

MATERIALS AND METHODS

Development of 591.1D7.34, a novel anti-CD13 monoclonal antibody (mAb). The investigations summarized in this report began as an approach to defining novel inflammatory pathways in RA involving FLS, triggered preferentially by IL-17 rather than by tumor necrosis factor α (TNFα). BALB/c mice were serially immunized with 10^6 FLS treated with 10 ng/ml IL-17 for 48 hours prior to immunization. A spleen from the most reactive mouse (assessed by flow cytometry of FLS using mouse sera) was fused to a nonsecreting myeloma cell line. The resulting hybridoma clones were screened on resting FLS and IL-17–treated FLS, and then subcloned. An osteoarthritis (OA) FLS cell line was biotinylated and lysed. Immunoprecipitation was used to isolate the protein recognized by mAb 591.1D7.34 (hereafter called 1D7). Controls included mouse IgG (isotype control) and anti-CD98. The eluted proteins were electrophoresed under reducing or nonreducing conditions on a 4–20% Tris–glycine polyacrylamide gel. The gel was transferred to an Immobilon-P membrane and incubated with streptavidin–horseradish peroxidase (HRP) (BioLegend) and then with ECL substrate (Pierce).

U937 myeloid cells were also lysed, and 1D7 was used to immunoprecipitate a protein which was resolved by electrophoresis on 2 identical polyacrylamide gels. One was stained with Coomassie blue, and the other was excised at a spot corresponding to the primary band in the stained gel. The protein was subjected to trypsin digestion in-gel, and the resulting peptide mixture was analyzed by liquid chromatography tandem mass spectrometry on a Qtof premier instrument (Waters). Protein Lynx Global Server and Mascot search engines were used to search the UniProt and NCBI databases. The protein identified matched aminopeptidase N/CD13.

Cell culture. Procedures involving specimens obtained from human subjects were performed under a protocol approved by the University of Michigan Institutional Review Board. Histologic evaluation of synovial tissues was performed as previously described (19). FLS from human synovial tissue obtained at arthroplasty or synovectomy from RA or OA joints were cultured following digestion with 1% collagenase and separation through a 70 μm cell strainer. The diagnosis of RA required at least 4 American College of Rheumatology 1987 revised criteria (20). The diagnosis of OA was based upon characteristic clinical and radiographic features. U937 cells were cultured in RPMI 1640 containing 10% fetal bovine serum (FBS), 2% L-glutamine, 1% HEPES, 1% sodium pyruvate, and 0.5% glucose. FLS were maintained in CMRL medium (20% FBS, 2 m*M* L-glutamine, 1% penicillin/streptomycin) and were used between passages 4 and 10. Cultures were moved to serum-free media (Dulbecco's modified Eagle's medium [DMEM]/F-12) with PeproGrow serum replacement (PeproTech) 2 days before harvesting. T cells were isolated from peripheral blood of healthy subjects using RosetteSep Human T cell enrichment cocktail (StemCell Technologies) and Histopaque (Sigma-Aldrich). Cytokine-activated T cells were prepared by culture of T cells in IL-6 (100 ng/ml), IL-2 (25 ng/ml), and TNFα (25 ng/ml) for 7–10 days in 10% FBS/RPMI 1640 medium (21,22). The COS-1 cell line (ATCC) was grown in 10% FBS/DMEM.

Sample preparation. SF samples were treated for 5 minutes with 0.05% bovine testis hyaluronidase (1 drop per 1 ml of fluid; Sigma-Aldrich). Cells were lysed in cell lysis buffer (10% Nonidet P40, 10% phenylmethylsulfonyl fluoride, 1% iodoacetamide, and 0.1% E-64 in trichostatin A) for 1 hour on ice. FLS culture supernatants were concentrated by centrifugation through an Amicon Ultracel 30K filter (Millipore).

Flow cytometry. Fibroblasts were removed from flasks by 3 m*M* EDTA in phosphate buffered saline (PBS). Cells were stained with mouse IgG (negative control) or anti-CD13 (1D7, SJ1D1 [Abcam], or WM15 [BioLegend]) and then with Alexa Fluor 488–conjugated goat anti-mouse IgG (Molecular Probes). Cytometry was performed on a FACSCalibur (BD Biosciences).

Aminopeptidase enzymatic activity. Aminopeptidase activity was measured by cleavage of L-leucine–7-amido-4-methyl-coumarin (L-leucine–AMC; Sigma-Aldrich) to release the fluorescent molecule AMC. A standard curve was constructed using AMC (Sigma-Aldrich). The assay was run in 0.1*M* Tris HCl buffer (pH 8.0). Samples were incubated with the substrate at 37°C for 1 hour and then read using a fluorescence plate reader at emission 450 nm, excitation 365 nm. Results were calculated as μM/hour of substrate cleaved.

CD13 enzyme-linked immunosorbent assay (ELISA). High-binding ELISA plates were coated overnight with the anti-CD13 monoclonal antibody WM15 in 0.1*M* carbonate buffer (pH 9.5) and blocked overnight with 1× Animal Free Block (Vector). Samples were then applied to the plates either

whole or diluted in block with 10 m*M* EDTA. The standard curve was prepared using recombinant human CD13 (R&D Systems) in block with 10 m*M* EDTA. The mAb 1D7 was biotinylated (Biotin-XX Microscale Protein Labeling kit; Molecular Probes) and applied overnight. Streptavidin–HRP was then added. Between steps, the plates were washed with PBS plus 0.05% Tween. The plates were visualized with tetramethylbenzidine substrate (BD Biosciences). The reaction was stopped with 2*M* H_2SO_4 and analyzed on a colorimetric plate reader.

Immunoprecipitation. Immunoprecipitation was performed using a Pierce Direct IP kit (Thermo Scientific). Briefly, antibodies (anti-CD13 [1D7], anti-CD98 [7F8] [23], or isotype control [mouse IgG]) were bound to AminoLink Plus beads (Thermo Scientific) using cyanoborohydride. Samples were diluted 1:1 with immunoprecipitation lysis/wash buffer and incubated overnight with the beads. The depleted portion was removed by centrifugation. Protein was eluted off the beads by low pH (2.8), which was neutralized with 1*M* Tris (pH 9.5).

Chemotaxis assay. The chemotaxis assay was a modified chemotaxis-under-agarose system (24,25). Some plates were coated overnight at 4°C with 10 μg/ml fibronectin then washed twice with PBS. A 2.4% agarose (UltraPure; Invitrogen) solution in 1× Hanks' balanced salt solution (HBSS) was boiled and combined with 2 parts 1% bovine serum albumin (BSA) in RPMI 1640 and 1 part 1× HBSS. Three milliliters of this solution was added to each well of a 6-well plate and allowed to cool to room temperature. A 3-hole punch (University of Michigan Instrument Shop) was used to create three 4-mm wells with edges 3 mm apart, and the plates were equilibrated to 37°C. Chemoattractants and T cells were adjusted to appropriate concentrations in chemotaxis medium (0.1% BSA, 2% L-glutamine, 1% penicillin/streptomycin, in RPMI 1640 without phenol red). Some cytokine-activated T cell samples were treated for 2 hours at 37°C with 100 ng/ml of pertussis toxin in 10% RPMI 1640, then washed once with 0.1% BSA in RPMI 1640 (viability ≥95%). T cells (2.5×10^5) were added to the center well. A medium-only control was added to an outside well, while the chemoattractant solution was added to the opposite outside well. Plates were incubated at 37°C in 5% CO_2 either overnight (uncoated) or for 5 hours (fibronectin coated). Pictures were taken of the area directly between the outside and center wells using an EVOS inverted microscope at 100× magnification. Cell counts were ln-transformed, and data are expressed as a chemotactic index (ln-transformed number of cells migrated to stimulus − ln-transformed number of cells migrated to medium alone).

CD13 enzymatic mutation. A CD13 clone (MGC Human ANPEP Sequence-Verified cDNA; GenBank accession no. BC058928) was obtained from Open Biosystems. An enzymatically inactive mutant CD13 (E355Q) was created. The plasmid (1 μg DNA) was linearized by double digestion with *Sgr* AI (2 units) and *Sbf* I (10 units) (New England Biolabs). The 7.3-kb fragment was purified from a 1% agarose gel using a QIAquick Gel Extraction kit (Qiagen). The plasmid fragment and 2 gene blocks from Integrated DNA Technologies (5′-TGGCCTGCCAGACTTCAACGCCGGCGCCATGCAGAACTGGGGACTGGTGACCTACCGGGAGAACTCCCTGCTGTTCGACCCCCTGTCCTCCTCCAGCAGCAACAAGGAGCGGGTGGTCACTGTGATTGCTCATGAGCTGGCCCACCAGTGGTTCGGGAACCTGGTGACCATAGAGTGGTGGAATGACCTGTGGCTGAACGAGGGCTTCGCCTCCTACGTGGAGTACCTGGGTGCTGACTATGCGGAGCCCACCTGGAACTTGAAAGACCTCATGGTGCTGAATGA-3′ and 5′-GACCTCATGGTGCTGAATGATGTGTACCGCGTGATGGCAGTGGATGCACTGGCCTCCTCCCACCCGCTGTCCACACCCGCCTCGGAGATCAACACGCCGGCCCAGATCAGTGAGCTGTTTGACGCCATCTCCTACAGCAAGGGCGCCTCAGTCCTCAGGATGCTCTCCAGCTTCCTGTCCGAGGACGTATTCAAGCAGGGCCTGGCGTCCTACCTCCACACCTTTGCCTACCAGAACACCATCTACCTGAACCTGTGGGACCACCTGCAGGAGGCTGTGAACAACCGGT-3′) were assembled and transformed into NEB 5-alpha *Escherichia coli* using a Gibson Assembly Cloning kit (New England Biolabs).

Clones were selected by ampicillin resistance, and several colonies were sequenced (University of Michigan Sequencing Core) to identify correct clones. Plasmids for wild-type (WT) CD13 or enzymatically inactive CD13 were grown and isolated using an EndoFree Plasmid Maxi Kit (Qiagen). Plasmids were transfected into COS-1 cells using Lipofectamine LTX with Plus Reagent (Life Technologies). Mock transfection with Lipofectamine alone was used as a control. Cultures were switched to serum-free SFM4CHO media (Thermo Scientific) 48 hours after transfection, and cultures were harvested 24 hours later.

Statistical analysis. Concentrations, percent remaining, and chemotactic index are expressed as the mean ± SEM. Enzymatic activity is expressed as the mean ± SD. Statistically significant chemotaxis was assessed by Student's paired *t*-test comparing the ln-transformed number of cells migrated to stimulus with the ln-transformed number of cells migrated to medium alone; an unpaired *t*-test was used between groups. Otherwise, significance was determined by Student's unpaired *t*-test, unless otherwise noted.

RESULTS

Identification of CD13 as an IL-17–induced protein on FLS. To identify a surface structure on FLS that was regulated by IL-17 independently of TNFα, IL-17–treated FLS were used to immunize BALB/c mice, and hybridoma clones were created. The clones were screened on resting FLS, IL-17–treated FLS, and TNFα-treated FLS. A hybridoma was selected that produced an antibody (591.1D7.34) that recognized an FLS surface protein up-regulated by IL-17 but not by TNFα at 48 hours (Figure 1A). Of the cell types tested, the monocytic cell line, U937, showed the strongest expression of the molecule identified by 1D7. We therefore used 1D7 to immunoprecipitate a protein from U937 cells that migrated on sodium dodecyl sulfate–polyacrylamide gel electrophoresis as a single band of 150 kd, and that was identified as CD13/aminopeptidase N by sequencing of multiple peptide fragments (Figures 1B and C).

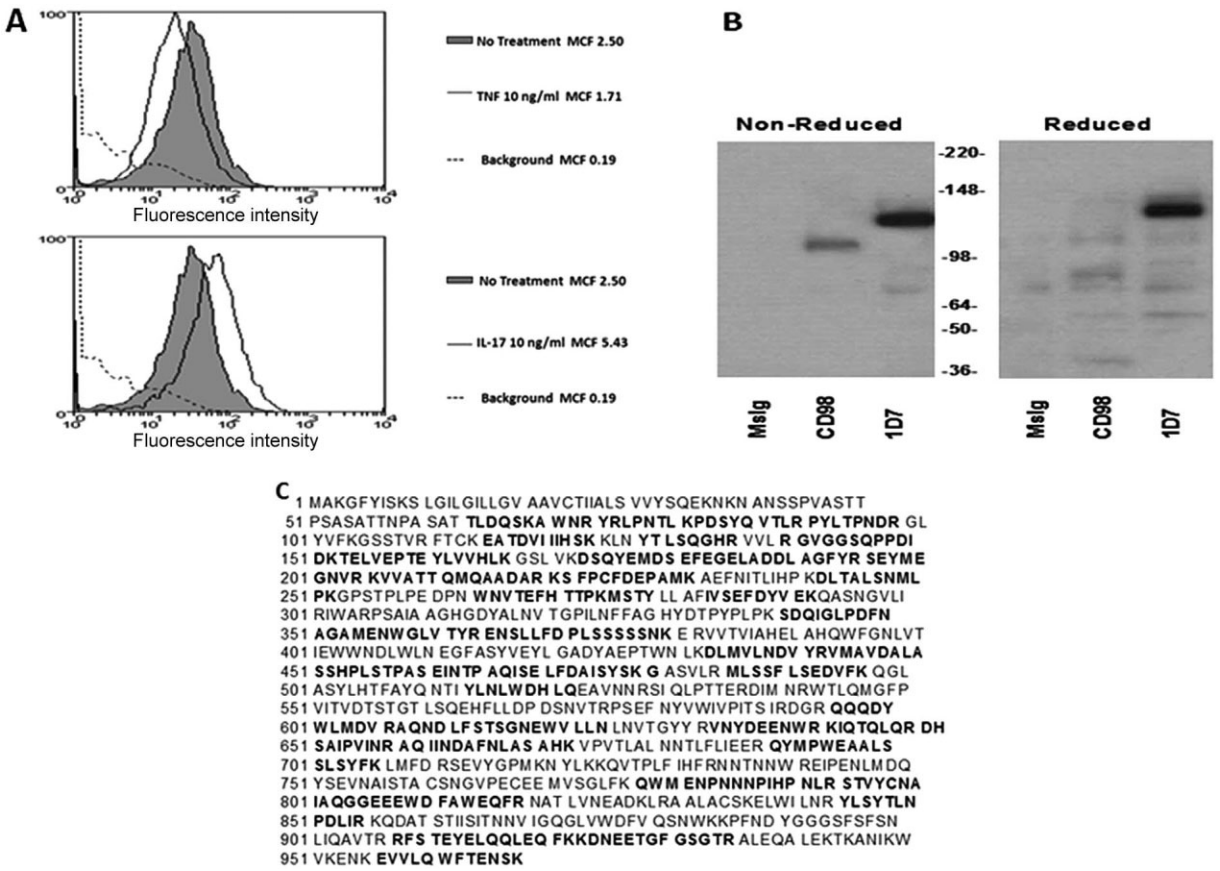

Figure 1. Identification of the protein recognized by monoclonal antibody 591.1D7.34 (1D7) and up-regulated by interleukin-17 (IL-17) as CD13. **A,** Fibroblast-like synoviocytes (FLS) were treated for 48 hours with medium alone, tumor necrosis factor α (TNFα), or IL-17 before staining with 1D7 and Alexa Fluor 488–conjugated goat anti-mouse IgG. MCF = mean channel fluorescence. **B,** An osteoarthritis FLS cell line was biotinylated and lysed. Immunoprecipitation was used to isolate protein recognized by 1D7, mouse IgG (MsIg; isotype control), or anti-CD98 antibodies that were bound to beads. Proteins eluted from the beads were resolved by sodium dodecyl sulfate–polyacrylamide gel electrophoresis under reducing or nonreducing conditions. Protein from the same number of cells was loaded in each lane. **C,** U937 myeloid cells were lysed, and 1D7 was used to immunoprecipitate the recognized protein, which was run on 2 gels. One was stained with Coomassie blue, and the other was excised at a spot corresponding to the primary band in the stained gel. The protein was extracted and multiple peptide fragments were sequenced, each of which matched portions of aminopeptidase N/CD13 (boldfaced sequences).

CD13 in RA in vivo. Having identified FLS CD13 as a potential part of an IL-17–induced pathway, we next sought to determine whether the concentration of a putative soluble form of CD13 was elevated in the RA joint. This was previously suggested by determination of levels of aminopeptidase activity in SF samples, but without direct measurement of CD13 protein (9,10). We developed a novel ELISA to measure CD13 in healthy control serum samples (n = 23), RA serum samples (n = 33), and both RA and OA SF samples (n = 98). RA SF samples (n = 39) had a mean ± SEM CD13 concentration of 1,191.09 ± 121.58 ng/ml with a mean ± SD activity of 3,402.45 ± 239.58 μM/hour, and OA SF samples (n = 59) had a mean ± SEM CD13 concentration of 646.11 ± 45.64 ng/ml and a mean ± SD activity of 2,250.28 ± 93.18 μM/hour (Figure 2A). RA SF samples had significantly higher concentration ($P < 0.00001$) and activity ($P < 0.00001$). The CD13 concentration in RA SF samples was also significantly higher than in the 33 RA serum samples (397.95 ± 72.18 ng/ml) ($P < 0.00001$) and significantly higher than in the 23 healthy control serum samples (683.34 ± 42.41 ng/ml) ($P = 0.0023$) (Figure 2B).The CD13 concentration was significantly higher in healthy control serum samples than in RA serum samples ($P = 0.0040$). The results are consistent with the observation that IL-17 up-regulates

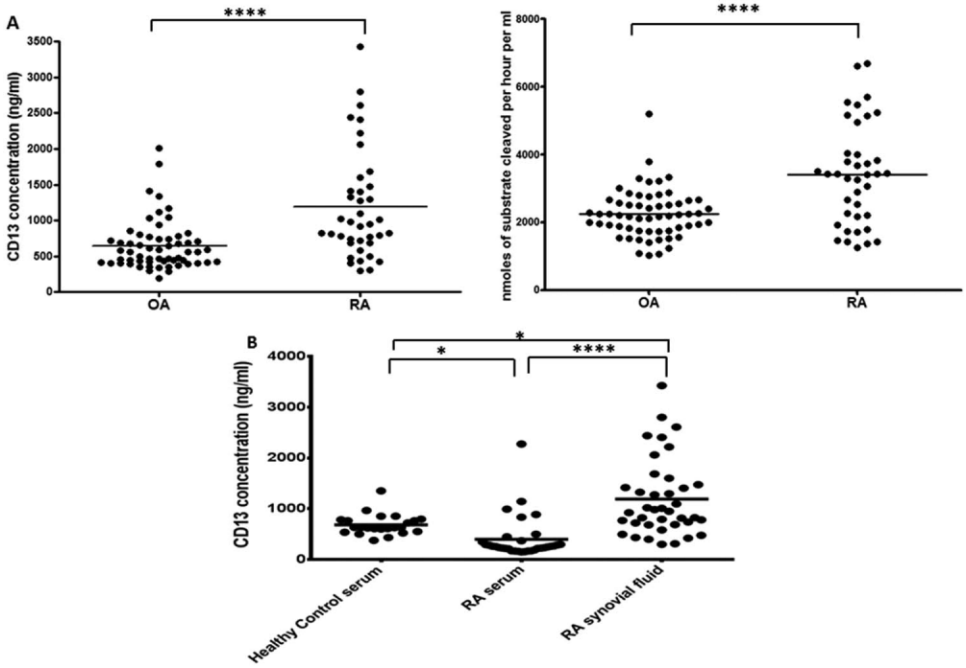

Figure 2. CD13 is found in vivo and its concentrations are higher in rheumatoid arthritis (RA) synovial fluid (SF) than in osteoarthritis (OA) SF. **A,** CD13 was measured by enzyme-linked immunosorbent assay (ELISA) in RA SF samples (n = 39) and OA SF samples (n = 59). CD13 enzymatic activity was measured in parallel. **B,** CD13 was measured by ELISA in sera from healthy controls (n = 23), in sera from RA patients (n = 33), and in SF samples from RA patients (n = 39; not matched to serum). Symbols represent individual samples; bars show the mean. $* = P < 0.05$; $**** = P < 0.00001$ by one-way analysis of variance.

CD13 expression by FLS and lead to the hypothesis that generation of sCD13 in the RA joint may play a role in a proinflammatory pathway.

CD13 on RA and OA FLS. Having identified CD13 on FLS and sCD13 in SF, we asked whether the difference between RA and OA SF samples corresponded to an increase in CD13 expression by RA FLS. We used antibodies WM15 and SJ1D1 in addition to 1D7 to measure CD13 by flow cytometry (Figure 3A). Each antibody detected CD13 on FLS, but with no significant difference in surface CD13 between resting RA FLS (n = 7) and resting OA FLS (n = 5). Moreover, measurement of total cell CD13 in lysates of RA and OA FLS by ELISA ($P = 0.74$) and enzymatic activity assay ($P = 0.15$) showed no significant differences (Figure 3B). In RA FLS, we found a CD13 concentration of 4,867.39 ± 1,196.81 ng/ml with an enzymatic activity of 2,993.65 ± 743.40 μM/hour, and in OA FLS, we found a CD13 concentration of 4,256.74 ± 1,306.71 ng/ml with an enzymatic activity of 2,123.05 ± 1,203.81 μM/hour. To determine whether FLS could release sCD13, we measured CD13 in FLS culture supernatants. FLS were cultured in serum-free media to eliminate interference from bovine CD13. Soluble CD13 was detected by ELISA in the supernatants and was enzymatically active, with almost identical results from RA FLS (51.28 ± 5.15 ng/ml, 957.69 ± 819.02 μM/hour) and OA FLS (50.78 ± 7.16 ng/ml, 962.69 ± 552.26 μM/hour) (Figure 3C).

CD13 and aminopeptidase activity in the joint. Although we found elevated levels of CD13 protein and enzymatic activity in RA in vivo, we did not find any differences in vitro between RA and OA FLS. We next sought to confirm that the N-aminopeptidase activity attributed to CD13 in SF samples was really due to CD13. The correlation between CD13 concentration and aminopeptidase activity in SF samples was $R^2 = 0.1365$ ($P = 4.24 \times 10^{-9}$ by analysis of variance [ANOVA]). Considering OA samples separately, the correlation remained highly significant ($R^2 = 0.418$, $P = 3.17 \times 10^{-8}$ by ANOVA). However, in RA samples, the correlation was not significant ($R^2 = 0.0947$, $P = 0.057$ by ANOVA) (Figure 4A). Several outliers could indicate the variable presence of other proteins with aminopep-

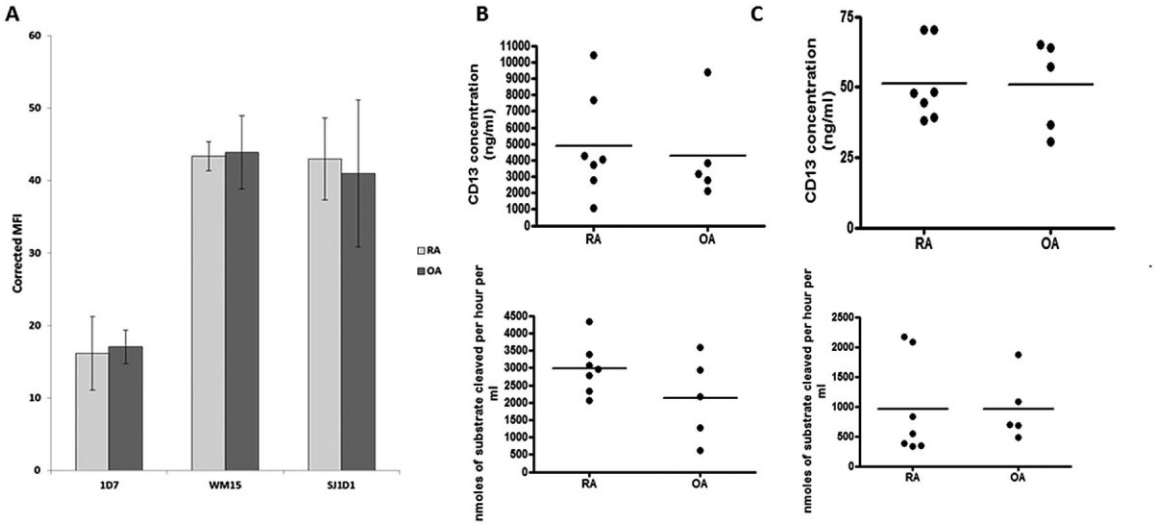

Figure 3. Equivalent expression of CD13 by RA fibroblast-like synoviocytes (FLS) and OA FLS. **A,** FLS were immunostained for CD13 using 3 antibodies (591.1D7.34 [1D7], WM15, SJ1D1) that recognize different epitopes. All 3 showed high expression. Mean fluorescence intensity (MFI) was adjusted for the isotype control as follows: MFI CD13 − MFI mouse IgG = corrected MFI. Values are the mean ± SD. **B,** RA FLS (n = 7) and OA FLS (n = 5) were grown to confluence in 20% CMRL medium and switched to serum-free media for 48 hours prior to harvesting. Cells were lysed, and CD13 was measured by ELISA and enzymatic activity assay. **C,** The 48-hour culture supernatants were concentrated from 25 ml to 1 ml through a 30-kd centrifugal filter and measured by ELISA and enzymatic activity assay. In **B** and **C,** symbols represent individual samples; bars show the mean. See Figure 2 for other definitions.

tidase activity. To further assess the issue, we immunodepleted RA SF samples (n = 6) and OA SF samples (n = 3) using 1D7 and assayed the depleted fractions for CD13 and aminopeptidase activity. Successful immunodepletion of CD13 (partial or complete) was verified by ELISA. We showed significant depletion of both CD13 protein (11.50 ± 0.26% remaining; $P = 0.00055$) and enzymatic activity (55.74 ± 0.31% remaining; $P = 0.0027$) (Figure 4B). In most SF samples, the remaining percentage of aminopeptidase activity was higher than the remaining percentage of CD13 protein. Moreover, 100% depletion of CD13 protein failed to remove all of the aminopeptidase activity.

An example in Figure 4C shows 1 RA SF sample with complete depletion of CD13 as measured by ELISA in which the enzymatic activity was 876.61 ± 36.06 μM/hour in the isotype control–treated sample and 356.00 ± 17.47 μM/hour in the CD13-depleted sample ($P = 2.3 \times 10^{-5}$). Much of the enzymatic activity in this sample appeared in the eluate from the 1D7 immunoprecipitation (3,888.00 ± 39.97 μM/hour). However, this only accounted for ~60% of the starting enzymatic activity.

Cytokine-activated T cell migration aided by recombinant human CD13. Having determined that CD13 is present in high amounts in SF and is enzymatically active, we next considered a possible function of CD13 in RA. Two previous reports suggested that CD13 is chemotactic for T cells (10,26). We sought to verify this observation and to determine whether CD13 could be chemotactic for cytokine-activated T cells, an in vitro–generated cell population that phenotypically and functionally resembles T cells found in RA synovium (21,22). We used a modified chemotaxis-under-agarose system with SDF-1/CXCL12 and TARC/CCL17 as positive controls. SDF-1 and TARC had chemotactic indices of 0.45 ± 0.23 ($P = 0.068$) and 0.42 ± 0.12 ($P = 0.0012$), respectively, without fibronectin and 0.88 ± 0.29 ($P = 0.0046$) and 0.46 ± 0.42 ($P = 0.28$), respectively, with fibronectin (Figure 5A). Recombinant human CD13 was used over a range of concentrations from 1,000 ng/ml to 50 ng/ml and was chemotactic for cytokine-activated T cells between 700 ng/ml and 50 ng/ml. Peak chemotaxis for CD13 was from 200 ng/ml (0.34 ± 0.29) to 500 ng/ml (0.50 ± 0.18) and was significantly greater than for medium alone (chemotactic index of zero) at both concentrations ($P = 0.029$ and $P = 0.0079$, respectively). Chemotaxis for recombinant human CD13 was also significant at 200 ng/ml with fibronectin coating (0.72 ± 0.29; $P = 0.018$) (Figure 5A). Representative images of the chemotaxis assays are

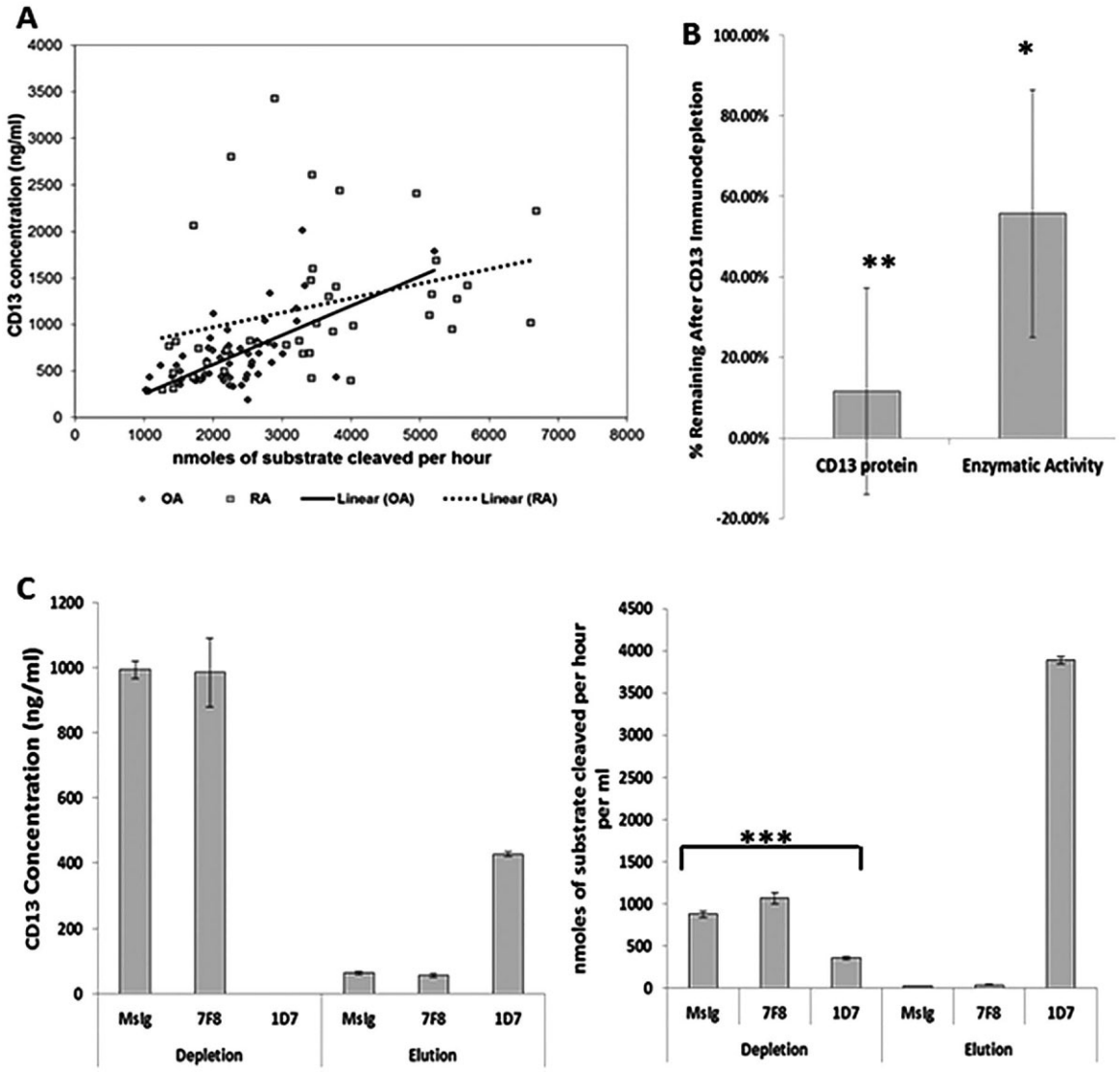

Figure 4. CD13 accounts for most but not all of the aminopeptidase activity in SF. **A,** ELISA and enzymatic activity assay results for RA SF samples and OA SF samples were correlated separately and together. Correlations were analyzed by analysis of variance: for all points together, $R^2 = 0.1365$, $P = 4.24 \times 10^{-9}$; for OA alone, $R^2 = 0.418$, $P = 3.17 \times 10^{-8}$; for RA alone, $R^2 = 0.0947$, $P = 0.057$. **B,** SF samples (n = 9) were immunodepleted with anti-CD13 (591.1D7.34 [1D7]), Ig isotype control (mouse IgG; MsIg), or an isotype-matched irrelevant antibody (anti-CD98 [7F8]). The removed protein was eluted off the beads by low pH. Values are the mean ± SEM. $* = P < 0.05$; $** = P < 0.001$ versus no immunodepletion, by unpaired 2-tailed *t*-test. **C,** Shown is an example of complete depletion of CD13 in an RA SF sample as measured by ELISA; also shown are corresponding enzymatic activity assay results (n = 1 RA SF sample with 3 replicated experiments). Values at left are the mean ± SEM; values at right are the mean ± SD. $*** = P < 0.0001$ by unpaired 2-tailed *t*-test. See Figure 2 for other definitions.

shown in Supplementary Figure 1 (available on the *Arthritis & Rheumatology* web site at http://onlinelibrary.wiley.com/doi/10.1002/art.38878/abstract).

CD13 contributes to chemotactic activity of SF independent of its enzymatic activity. We next investigated whether CD13 contributes to the chemotactic potential of RA SF. To test for a potential role of CD13 in cytokine-activated T cell chemotaxis, we immunodepleted SF samples from 3 different random donors with anti-CD13 (1D7) or mock-depleted them with an isotype control (mouse IgG). The mock-depleted SF samples had a chemotactic index of 1.37 ± 0.44, which was significantly chemotactic ($P = 0.0065$). Immunodepleting CD13 from the SF samples resulted in a significant

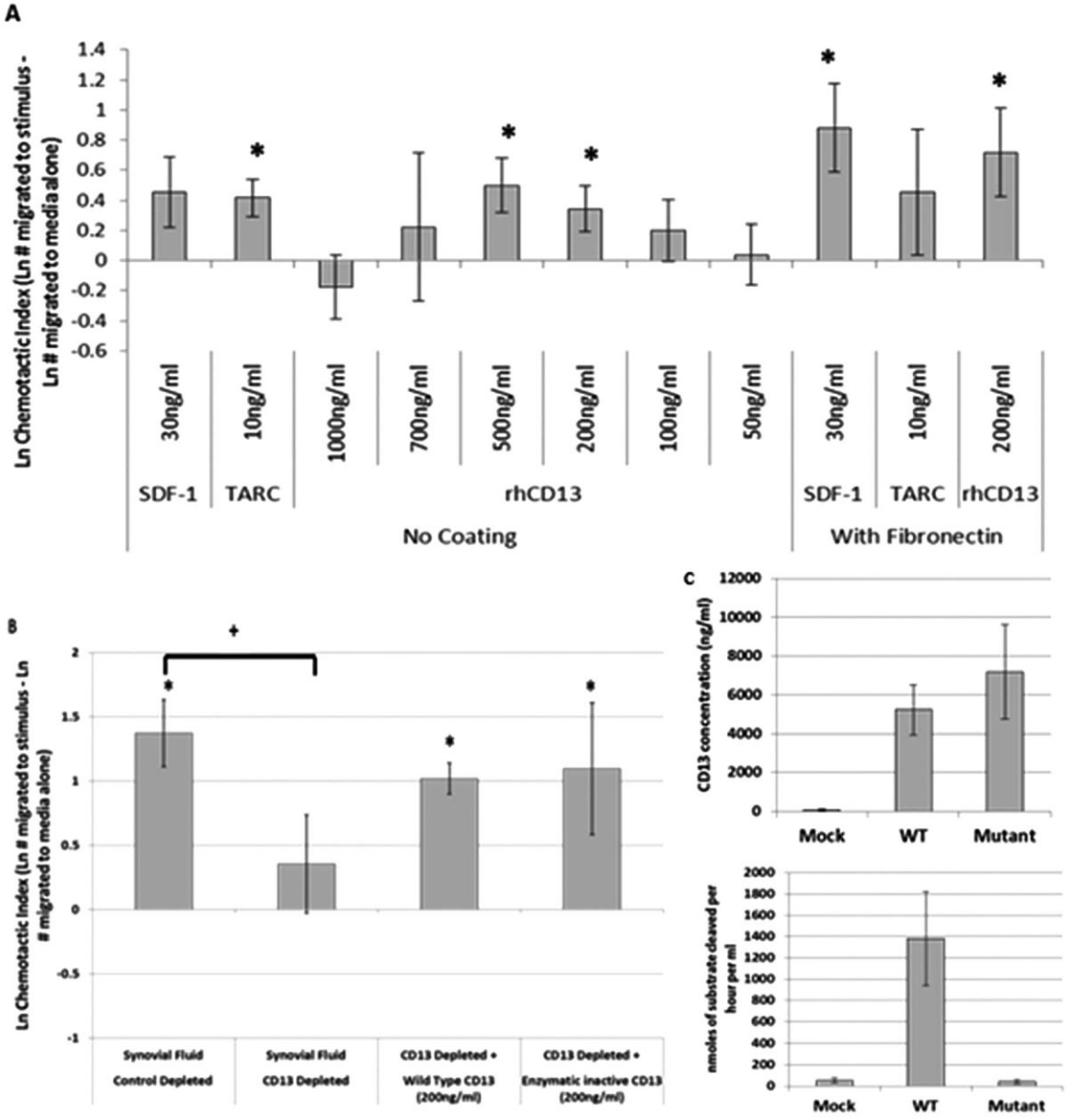

Figure 5. CD13 is chemotactic for cytokine-activated T cells independent of its enzymatic activity. Cytokine-activated T cells were placed in the center well of a chemotaxis-under-agarose system with a medium-only control in one of the side wells and a chemotactic agent in the opposite well. Some plates were coated with fibronectin. **A,** Positive wells were loaded with recombinant human CD13 (rhCD13) or with the chemotactic controls stromal cell–derived factor 1 (SDF-1)/CXCL12 or thymus and activation–regulated chemokine (TARC)/CCL17 ($n \geq 12$ samples per group). Values are the mean ± SEM. **B,** Positive wells were loaded with SF samples from 3 different random donors. Samples were immunodepleted with anti-CD13 (591.1D7.34 [1D7]) or mock-depleted (Mock) with an isotype control (mouse IgG) at a 1:10 dilution. In addition, CD13-depleted SF samples were supplemented with supernatant from transfected COS-1 cells containing wild-type (WT) CD13 or enzymatically inactive mutant CD13 ($n \geq 19$ samples per group). Cell counts were ln-transformed and data are expressed as a chemotactic index (ln-transformed number of cells migrated to stimulus − ln-transformed number of cells migrated to medium alone). Values are the mean ± SEM. $* = P < 0.05$ versus medium alone, by paired 2-tailed *t*-test. $+ = P < 0.05$ by unpaired 2-tailed *t*-test. **C,** The concentration of CD13 in the COS-1 supernatants was determined by ELISA and was used at 200 ng/ml in assays shown in **B**. Values are the mean ± SEM. Enzymatic activity was measured by N-aminopeptidase activity assay. Values are the mean ± SD. See Figure 2 for other definitions.

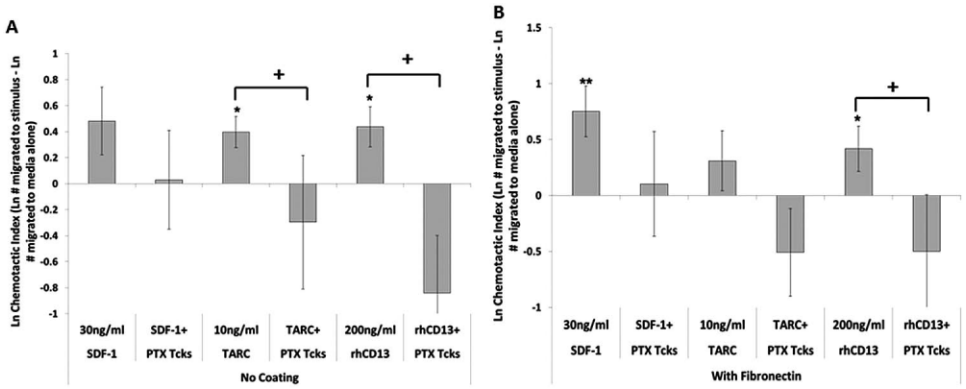

Figure 6. CD13 chemotaxis functions through a pertussis toxin (PTX)–sensitive G protein–coupled receptor. Cytokine-activated T cells (Tcks) were placed in the center well of a chemotaxis-under-agarose system with a media-only negative control in one of the side wells and a chemotactic agent (SDF-1, TARC, or recombinant human CD13) at the indicated concentration in the opposite well. Plates were left untreated (**A**) or were coated overnight with 10 μg/ml fibronectin (**B**). Some cytokine-activated T cells were treated with 100 ng/ml of pertussis toxin for 2 hours at 37°C ($n \geq 20$ samples per group). Cell counts were ln-transformed and data are expressed as a chemotactic index (ln-transformed number of cells migrated to stimulus − ln-transformed number of cells migrated to medium alone). Values are the mean ± SEM. $* = P < 0.05$; $** = P < 0.001$ versus medium alone, by paired 2-tailed *t*-test. $+ = P \leq 0.05$ by unpaired 2-tailed *t*-test. See Figure 5 for other definitions.

decrease in chemotaxis (to a chemotactic index of 0.35 ± 0.21) ($P = 0.041$) (Figure 5B).

We next examined whether the chemotactic ability of CD13 required its enzymatic activity. COS-1 cells were used to express plasmids containing either WT CD13 or an enzymatically inactive mutant CD13 (E355Q) (27). The CD13 ELISA was used to measure CD13 concentration, and loss of enzymatic activity in the mutant was confirmed by the N-aminopeptidase assay (Figure 5C). We supplemented CD13-depleted SF samples with 200 ng/ml of either WT or mutant CD13 from the COS-1 supernatants, both of which partially restored the chemotactic activity of the depleted SF samples to a similar level. WT CD13 increased the chemotactic index from 0.35 ± 0.21 to 1.02 ± 0.31, and mutant CD13 increased the chemotactic index to 1.10 ± 0.30, each representing significant chemotaxis compared with medium alone ($P = 0.0031$ and $P = 0.0018$, respectively) (Figure 5B).

Chemotaxis of T cells initiated by CD13 through a G protein–coupled receptor (GPCR). Most known chemokines function through a GPCR (28). We used pertussis toxin to determine whether the mechanism for CD13-induced chemotaxis functions similarly. Pertussis toxin treatment of cytokine-activated T cells significantly reduced chemotaxis for 200 ng/ml of recombinant human CD13 either with a fibronectin coating (from 0.42 ± 0.20 to −0.50 ± 0.50; $P = 0.047$) or without (from 0.44 ± 0.15 to −0.84 ± 0.44; $P = 0.00096$) and also inhibited migration toward SDF-1 and TARC-positive controls (significant for TARC, uncoated, at $P = 0.05$) (Figure 6).

DISCUSSION

It has become clear that RA is not mediated by a single cell type but rather by interactions between the various cells in the RA joint, including FLS and T cells. RA FLS express matrix metalloproteinases, secrete proinflammatory mediators, and produce chemotactic agents to attract inflammatory cells to the joint. T cells are prime producers of multiple proinflammatory cytokines (such as IL-17, TNFα, and interferon-γ). We explored the potential role of CD13, which is highly expressed on FLS, as one possible factor in the FLS–T cell interactions.

Although CD13 has been identified in synovial fluids by Western blotting and through N-aminopeptidase enzymatic activity assays, it has never been directly measured. We developed a novel CD13 ELISA and showed that CD13 concentrations are significantly higher in RA SF than in OA SF, healthy control sera, or RA sera. We also noted a significantly higher concentration of CD13 in healthy control sera when compared to RA sera (Figure 2). This could represent an influx of CD13-expressing cells (such as monocytes) into the joint, leaving fewer circulating CD13-shedding cells. We observed higher costaining of CD13 and a monocytic lineage marker (CD11c) in RA synovial tissues than in OA or normal synovial tissues

(see Supplementary Figure 2, available on the *Arthritis & Rheumatology* web site at http://onlinelibrary.wiley.com/doi/10.1002/art.38878/abstract). We were specifically interested in whether FLS could contribute to the sCD13 we found in SF. FLS strongly express surface CD13 and are therefore a logical choice for shedding of CD13. We were able to show that sCD13 does come from FLS (Figure 3C) (see Supplementary Figure 2), and we can thereby infer that FLS contribute to the sCD13 in SF. We expected that CD13 would be elevated on RA FLS as compared to OA FLS, as previously reported (10). However, our data showed no noticeable difference (Figure 3). We noted a large variation in the intensity of CD13 expression on our cell lines and in SF and serum samples. We believe that this variation may account for the differences between our results and those previously reported (10).

There are at least 4 possible explanations for the higher amount of sCD13 in RA SF than in OA SF. First, the RA joint environment includes cytokines and growth factors that could up-regulate CD13 expression or release from FLS in vivo in a manner that might not be maintained in vitro (13). This is supported by our finding that IL-17 increases surface expression of CD13 (Figure 1A). Second, synovial tissue undergoes hyperplasia in RA, resulting in much higher numbers of FLS that could release CD13. Third, the increase could be due to other cell types. Endothelial cells and cells of the monocytic cell lineage express surface CD13 (2–4). These cells are often found in higher numbers in the RA joint and so could account for the increased sCD13. Finally, there is increased expression of proteases in RA synovium, which could increase shedding of CD13 from FLS (29). The most likely explanation for the higher sCD13 in RA SF combines all 4 possibilities. The complex milieu present in the RA joint contributes to the higher numbers of FLS and other cells as well as the regulation and shedding of CD13 from those cells, although monocytic shedding of CD13 has only been observed previously in apoptotic cells (30).

We wanted to ensure that the aminopeptidase activity we were measuring could be attributed to CD13. The mAb 1D7 was used for immunodepletion since it does not block enzymatic activity (data not shown). We found that CD13 contributes the majority of N-aminopeptidase activity to SF; however, it appears that at least 1 other protein present has similar activity (Figures 4B and C) (5). The correlation analysis (Figure 4A) showed a few SF samples that also appeared to have a high concentration of CD13 but lower enzymatic activity. This could indicate the presence of natural inhibitors and/or intrinsic differences in the CD13 protein from posttranslational modifications, resulting in differing degrees of enzymatic activity.

It was previously suggested that CD13 may act as a chemokine for T cells (10,26). We wanted to further explore this function as one possible aspect of the interaction between FLS and T cells in the RA joint. We tested for chemotaxis with SDF-1, TARC, or recombinant human CD13 using not only cytokine-activated T cells, but also resting T cells, anti-CD3/CD28–activated cells, Jurkat cells, HUT-78 cells, and mitogen-activated T cells (data not shown). We chose cytokine-activated T cells because we achieved the most consistent and significant chemotaxis with both positive control chemokines and recombinant human CD13 with this cell type. This is of particular interest as cytokine-activated T cells phenotypically resemble T cells found in the RA joint (19). Chemotaxis assays with recombinant human CD13 were performed over both a fibronectin-coated plate and an uncoated plate, to explore both a basic chemotaxis function (uncoated) and a matrix invasion–type function (fibronectin coating). Fibronectin improved adhesion of the cells to the plate, magnifying both specific and nonspecific movement. Even though recombinant human CD13 and SF were significantly chemotactic in both systems, each of the 2 known T cell chemokines (TARC and SDF-1) was significantly chemotactic in only 1 of the systems. Nevertheless, the chemotactic index was similar in both assays, and the results of these assays are subject to the effects of high nonspecific background movement.

It is important to note that the optimal levels of CD13 in the chemotaxis assays corresponded to sCD13 levels found in vivo, indicating that this process is likely biologically relevant (Figure 5A). Although the average CD13 concentration in RA SF is higher than the peak chemotactic range, it is possible that this serves to create a gradient between the joint and the serum with the high concentration in the joint aiding in T cell retention. Consistent with this notion, the average concentration of CD13 in OA SF was found to be similar to its concentration in normal serum (Figure 2).

It is known that there are multiple chemokines that contribute to the migration of T cells to the RA joint (31,32). Notwithstanding the effects of other chemokines, CD13 appears to contribute significantly to the chemotactic activity of SF, as cytokine-activated T cell chemotaxis decreases when CD13 is depleted from such samples (Figure 5B). CD13 has been shown to be able to regulate other chemokines, but in vitro studies with recombinant human CD13 indicate that CD13 can

initiate chemotaxis directly (33–36). To determine whether the CD13-dependent chemotaxis in SF occurred directly or through enzymatic effects on other molecules, we introduced recombinant human CD13 into the depleted SF samples using either WT CD13 or an enzymatically inactive mutant CD13 (E355Q). This residue is part of the highly conserved GAMEN motif that is involved in substrate binding (37,38). Both the WT and mutant CD13 proteins were able to partially restore chemotactic activity to a similar degree, demonstrating that the mechanism of chemotaxis is independent of enzymatic activity of CD13 (Figure 5B). This also indicates that CD13 likely binds directly to a receptor on the T cells. To confirm this, we used pertussis toxin–treated cytokine-activated T cells. Pertussis toxin is known to inhibit cellular responses mediated through $G_{i/o}$ proteins, including most chemokine receptors (28,39). We were able to show that CD13 also acts through a pertussis toxin–sensitive GPCR (Figure 6). We also saw similar results with a fibronectin coating, indicating a similar mechanism for basic chemotaxis or migration involving ECM.

Although we have defined one mechanism for CD13-mediated T cell chemotaxis in RA, CD13 in the RA joint is also likely involved in cleaving chemokines, ECM proteins, and other molecules that regulate migration of T cells and interaction of those T cells with FLS. Future investigation of these aspects of CD13 function and definition of the T cell receptor for CD13 will yield additional insights into the roles of CD13 in RA.

AUTHOR CONTRIBUTIONS

All authors were involved in drafting the article or revising it critically for important intellectual content, and all authors approved the final version to be published. Dr. Fox had full access to all of the data in the study and takes responsibility for the integrity of the data and the accuracy of the data analysis.

Study conception and design. Morgan, Endres, Urquhart, Chung, Fox.
Acquisition of data. Morgan, Endres, Behbahani-Nejad, Phillips, Ruth, Edhayan, Lanigan, Fox.
Analysis and interpretation of data. Morgan, Behbahani-Nejad, Ruth, Friday, Fox.

REFERENCES

1. Look AT, Ashmun RA, Shapiro LH, Peiper SC. Human myeloid plasma membrane glycoprotein CD13 (gp150) is identical to aminopeptidase N. J Clin Invest 1989;83:1299–307.
2. Riemann D, Kehlen A, Langner J. CD13: not just a marker in leukemia typing [review]. Immunol Today 1999;20:83–8.
3. Luan Y, Xu W. The structure and main functions of aminopeptidase N. Curr Med Chem 2007;14:639–47.
4. Mina-Osorio P. The moonlighting enzyme CD13: old and new functions to target [review]. Cell 2008;14:361–71.
5. Favaloro EJ, Browning T, Facey D. CD13 (GP150; aminopeptidase-N): predominant functional activity in blood is localized to plasma and is not cell-surface associated. Exp Hematol 1993;21:1695–701.
6. Watanabe Y, Ito K, Iwaki-Egawa S, Yamaguchi R, Fujimoto Y. Aminopeptidase N in sera of healthy subjects is a different n-terminal processed derivative from the one obtained from maternal serum. Mol Genet Metab 1998;63:289–94.
7. Larsen SL, Pedersen LO, Buus S, Stryhn A. T cell responses affected by aminopeptidase N (CD13)-mediated trimming of major histocompatibility complex class II-bound peptides. J Exp Med 1996;184:183–9.
8. Saiki I, Fujii H, Yoneda J, Abe F, Nakajima M, Tsuruo T, et al. Role of aminopeptidase N (CD13) in tumor-cell invasion and extracellular matrix degradation. Int J Cancer 1993;54:137–43.
9. Dan H, Tani K, Hase K, Shimizu T, Tamiya H, Biraa Y, et al. CD13/aminopeptidase N in collagen vascular diseases. Rheumatol Int 2003;23:271–6.
10. Shimizu T, Tani K, Hase K, Ogawa H, Huang L, Shinomiya F, et al. CD13/aminopeptidase N–induced lymphocyte involvement in inflamed joints of patients with rheumatoid arthritis. Arthritis Rheum 2002;46:2330–8.
11. Kitko CL, Levine JE, Storer BE, Chai X, Fox D, Braun TM, et al. Plasma CXCL9 elevations correlate with chronic GVHD diagnosis. Blood 2014;123:786–93.
12. Thielitz A, Ansorge S, Bank U, Tager M, Wrenger S, Gollnick H, et al. The ectopeptidases dipeptidyl peptidase IV (DP IV) and aminopeptidase N (APN) and their related enzymes as possible targets in the treatment of skin diseases. Front Biosci 2008;13:2364–75.
13. Lundy SK, Sarkar S, Tesmer LA, Fox DA. Cells of the synovium in rheumatoid arthritis: T lymphocytes [review]. Arthritis Res Ther 2007;9:202.
14. Van Hamburg JP, Asmawidjaja PS, Davelaar N, Mus AM, Colin EM, Hazes JM, et al. Th17 cells, but not Th1 cells, from patients with early rheumatoid arthritis are potent inducers of matrix metalloproteinases and proinflammatory cytokines upon synovial fibroblast interaction, including autocrine interleukin-17A production. Arthritis Rheum 2011;63:73–83.
15. Kim KW, Cho ML, Kim HR, Ju JH, Park MK, Oh HJ, et al. Up-regulation of stromal cell–derived factor 1 (CXCL12) production in rheumatoid synovial fibroblasts through interactions with T lymphocytes: role of interleukin-17 and CD40L–CD40 interaction. Arthritis Rheum 2007;56:1076–86.
16. Szekanec Z, Koch AE, Tak PP. Chemokine and chemokine receptor blockade in arthritis, a prototype of immune-mediated inflammatory diseases [review]. Neth J Med 2011;69:356–66.
17. Ruth JH, Rottman JB, Katschke KJ Jr, Qin S, Wu L, LaRosa G, et al. Selective lymphocyte chemokine receptor expression in the rheumatoid joint. Arthritis Rheum 2001;44:2750–60.
18. Scornik OA, Botbol V. Bestatin as an experimental tool in mammals. Curr Drug Metab 2001;2:67–85.
19. Isozaki T, Ruth JH, Amin MA, Campbell PL, Tsou PS, Ha CM, et al. Fucosyltransferase 1 mediates angiogenesis, cell adhesion and rheumatoid arthritis synovial tissue fibroblast proliferation. Arthritis Res Ther 2014;16:R28.
20. Arnett FC, Edworthy SM, Bloch DA, McShane DJ, Fries JF, Cooper NS, et al. The American Rheumatism Association 1987 revised criteria for the classification of rheumatoid arthritis. Arthritis Rheum 1988;31:315–24.
21. Brennan FM, Hayes AL, Ciesielski CJ, Green P, Foxwell BM, Feldmann M. Evidence that rheumatoid arthritis synovial T cells are similar to cytokine-activated T cells: involvement of phosphatidylinositol 3-kinase and nuclear factor κB pathways in tumor necrosis factor α production in rheumatoid arthritis. Arthritis Rheum 2002;46:31–41.
22. Bryant J, Ahern DJ, Brennan FM. CXCR4 and vascular cell adhesion molecule 1 are key chemokine/adhesion receptors in the

migration of cytokine-activated T cells. Arthritis Rheum 2012;64: 2137–46.
23. Freidman AW, Diaz LA Jr, Moore S, Schaller J, Fox DA. The human 4F2 antigen: evidence for cryptic and noncryptic epitopes and for a role of 4F2 in human T lymphocyte activation. Cell Immunol 1994;154:253–63.
24. Nelson RD, Quie PG, Simmons RL. Chemotaxis under agarose: a new and simple method for measuring chemotaxis and spontaneous migration of human polymorphonuclear leukocytes and monocytes. J Immunol 1975;115:1650–6.
25. Heit B, Kubes P. Measuring chemotaxis and chemokinesis: the under-agarose cell migration assay. Sci STKE 2003;2003:PL5.
26. Tani K, Ogushi F, Huang L, Kawano T, Tada H, Hariguchi N, et al. CD13/aminopeptidase N, a novel chemoattractant for T lymphocytes in pulmonary sarcoidosis. Am J Respir Crit Care Med 2000;161:1636–42.
27. Luciani N, Marie-Claire C, Ruffet E, Beaumont A, Roques BP, Fournie-Zaluski MC. Characterization of Glu^{350} as a critical residue involved in the N-terminal amine binding site of aminopeptidase N (EC 3.4.11.2): insights into its mechanism of action. Biochemistry 1998;37:686–92.
28. Allen SJ, Crown SE, Handel TM. Chemokine: receptor structure, interactions, and antagonism. Annu Rev Immunol 2007;25: 787–820.
29. Mantle D, Falkous G, Walker D. Quantification of protease activities in synovial fluid from rheumatoid and osteoarthritis cases: comparison with antioxidant and free radical damage markers. Clin Chim Acta 1999;284:45–58.
30. Brown SB, Kluck RM, Ellem KA. Loss and shedding of surface markers from the leukemic myeloid monocytic line THP-1 induced to undergo apoptosis. J Cell Biochem 1996;60:246–59.
31. Miossec P, Dinarello CA, Ziff M. Interleukin-1 lymphocyte chemotactic activity in rheumatoid arthritis synovial fluid. Arthritis Rheum 1986;29:461–70.
32. Al-Mughales J, Blyth TH, Hunter JA, Wilkinson PC. The chemoattractant activity of rheumatoid synovial fluid for human lymphocytes is due to multiple cytokines. Clin Exp Immunol 1996;106:230–6.
33. Kanayama N, Kajiwara Y, Goto J, Maradny EE, Maehara K, Andou K, et al. Inactivation of interleukin-8 by aminopeptidase N (CD13). J Leukoc Biol 1995;57:129–34.
34. Wulfaenger J, Niedling S, Riemann D, Seliger B. Aminopeptidase N (APN)/CD13-dependent CXCR4 downregulation is associated with diminished cell migration, proliferation, and invasion. Mol Membr Biol 2008;25:72–82.
35. Chomarat P, Rissoan MC, Pin JJ, Banchereau J, Miossec P. Contribution of IL-1, CD14, and CD13 in the increased IL-6 production induced by in vitro monocyte-synoviocyte interactions. J Immunol 1995;155:3645–52.
36. Proost P, Mortier A, Loos T, Vandercappellen J, Gouwy M, Ronsse I, et al. Proteolytic processing of CXCL11 by CD13/aminopeptidase N impairs CXCR3 and CXCR7 binding and signaling and reduces lymphocyte and endothelial cell migration. Blood 2007;110:37–44.
37. Wong AH, Zhou D, Rini JM. The X-ray crystal structure of human aminopeptidase N reveals a novel dimer and the basis for peptide processing. J Biol Chem 2012;287:36804–13.
38. Ashmun RA, Shapiro LH, Look AT. Deletion of the zinc-binding motif of CD13/aminopeptidase N molecules results in loss of epitopes that mediate binding of inhibitory antibodies. Blood 1992;79:3344–49.
39. Mangmool S, Kurose H. $G_{i/o}$ protein-dependent and -independent actions of pertussis toxin (PTX). Toxins (Basel) 2011;3:884–99.